Modeling the effect of intra-axonal heterogeneity on the action potential conduction

Giorgia Del Missier (6292403), Jarno Koetsier (6188513),
Max L. Jacobs (6296498), Xenia Sterl (6292950)

Research project 2
Master Systems Biology
Maastricht University
July 1, 2022

Word count: 4411

Graphical Abstract

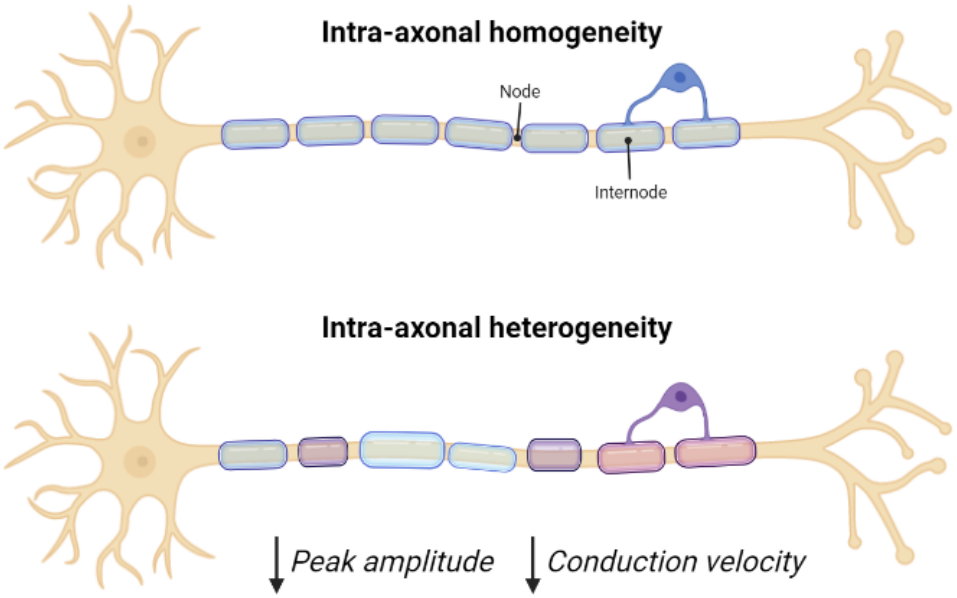

In brief, we show that variation in myelination along a single axon can significantly reduce the peak amplitude and conduction velocity. The differences in peak amplitude and conduction velocity between the heterogeneously myelinated axons are mainly explained by the small differences in mean myelination level and not by the distinct distribution of myelination along the axon.

1 Introduction

1.1 The axo-myelin unit

Rapid and efficient propagation of action potentials (APs) is an essential component of proper neuronal function and delivery of information throughout the nervous system, especially over long distances. In vertebrates, this is highly facilitated by myelin, a lipid-rich membrane enclosing the axon and isolating it from the extracellular space, acting as an electrical insulator.

Myelin is formed in layers by oligodendrocytes in the central nervous system, and by Schwann cells in the peripheral nervous system [1]. Along the axon, these myelin sheaths are interspaced by the nodes of Ranvier, where the axonal membrane is in direct contact with the extracellular space (Figure 1), allowing Na^+ and K^+ ions to cross the axonal membrane through the respective voltage-gated ion channels, generating a voltage trace of the distinct AP shape [1, 2]. This axonal geometry reduces the current flow across the axon by reducing its capacitance and increasing its resistance, providing the structural basis for fast, saltatory AP propagation from node to node

[3]. As a consequence, signal conduction is accelerated 20 to 100-fold when compared to non-myelinated axons of the same diameter [4]. Furthermore, this mechanism of saltatory movement of nerve impulses is metabolically efficient, as it eliminates the need for AP regeneration at every point of the axonal membrane [3].

Close communication between axons and myelinating glial cells is required for sheath formation and the regulation of myelin thickness. Additionally, reciprocal axo-glial signaling affects the axonal cytoskeleton and is needed for axonal survival. The result of this close interaction is the differentiation of the axonal membrane into distinct molecular, structural, and functional domains: the nodes of Ranvier, the paranodes, the juxtaparanodes, and the internodal regions [1–3, 5].

The common theory that myelin would act as a perfect insulator along the internodal regions has become progressively challenged by extended models based on experimental data. In fact, sharp-electrode intracellular recordings [6–8] and computer simulations [9–11] both provided evidence for axial current in the fluid-filled periaxonal and paranodal spaces. Recently, Cohen *et al.* (2020) were also able to prove the existence of this current experimentally, showcasing the importance of the many complex structures found along the axon [12].

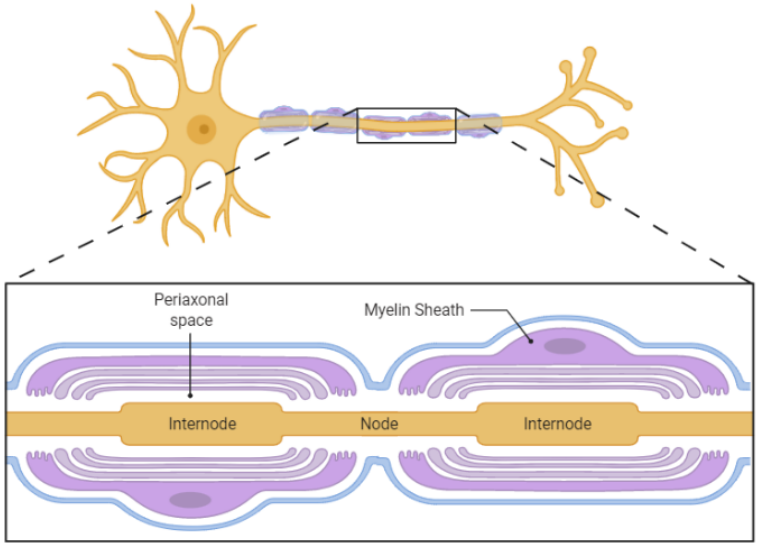

Figure 1: *Schematic representation of a myelin-covered neuron. Image created in BioRender.*

1.2 Computational approaches

Computational neuron models have proved to be of great value for efficiently and easily studying neuronal responses to varying stimuli. To represent the myelin sheath around axons in these models, three different approaches of increasing complexity can be found in the literature [11].

The first approach treats the myelin sheath as a perfect insulator of the internodal axolemma [13]. This can be modeled by a single-cable equivalent electrical circuit, in which the internodal segments consist of a single resistor to represent the axoplasm. The axon and myelin sheath here

form one tightly combined membrane, with no intermediary conducting pathways [12]. Although this is the most common representation of myelin, it lacks biological relevance, as it has been experimentally demonstrated that current flow through the myelin is possible [13].

The second approach to modeling myelin sheaths does allow some current flow through the myelin. This can also be modeled using a single-cable equivalent electrical circuit, with a series of compartments consisting of the parallel combination of a resistor and a capacitator representing the myelin [11].

Lastly, the third approach is to use a double-cable equivalent electrical circuit model, containing representations of nodes, paranodes, myelin, and axolemma. While the myelin is represented as described in the second approach, the internode is represented by two compartmental layers: the axon and the periaxonal space. Contrary to the other two described modeling frameworks, this approach can reproduce depolarising afterpotentials, which are thought to occur as a result of passive axolemma capacitance discharge [10]. Additionally, multiple other studies have shown the ability of this model to produce biologically accurate outputs [14], and successfully address a variety of biological questions. For example, it has contributed to the discovery that the length of the node of Ranvier can regulate the conduction speed of APs in myelinated axons [9, 15]. Thus, due to its proven increased biological accuracy, the double-cable model will be used in this study.

1.3 Research Question

Most modeling studies that use the double-cable model assume intra-axonal structural homogeneity [9, 12, 15–17]. Particularly, these studies commonly use a single parameter value to describe the length of *all* internodes in the model. Similarly, myelin thickness and periaxonal space width are also often assumed to be homogeneously distributed along the axon. In reality, however, these may vary significantly along the length of the axon. Specifically, myelination of neurons has been shown to be a highly dynamic process characterized by variable growth and remodeling across the axon [18]. Furthermore, axons in the cortex, as well as the auditory and visual systems, have been demonstrated to exhibit specific patterns of irregular myelination [15, 19, 20]. However, it is yet unclear how this heterogeneity of myelination patterns (*e.g.*, internode length, myelin thickness, and periaxonal space width) along the axon affects AP propagation.

In this study, we, therefore, aim to investigate the effect of intra-axonal variation of the internode length, myelin thickness, and periaxonal space width on the AP shape and conduction velocity using the double-cable model. Since intra-axonal myelin plasticity is involved in regulating AP conduction, we hypothesize that incorporating these variations into the double-cable model will significantly change the conduction velocity and the shape of the voltage trace of the AP when compared to the model without intra-axonal heterogeneity.

1.4 Innovation & Significance

Previous computational modeling studies have demonstrated the effect of varying internode length [9], periaxonal space width [16], and myelin thickness [17] on AP conduction. However, these studies always made use of the same parameter values for all internodes included in the model. Thus, to the best of our knowledge, no previous research has focused on how intra-axonal variation of the internode length, periaxonal space width, and myelin thickness collectively affects AP shape and conduction velocity. Our innovative research aims at developing a new framework for computational neuroscience by incorporating intra-axonal heterogeneity into the double-cable model. Our final aim is to investigate whether variable values of myelination parameters along the length of the axon have a clear effect on AP shape and conduction velocity, and thus possibly to establish the need of incorporating this variation in future developments of the model in order to further increase its biological accuracy.

Learning about the effects of intra-axonal heterogeneity on the AP shape and propagation velocity might provide valuable insight into how intra-axonal myelin plasticity can regulate neuronal signal conduction in the healthy brain. An enhanced understanding of axo-myelin plasticity is also essential for a better understanding of dys- and demyelinating disorders. Multiple sclerosis and metachromatic leukodystrophy are just two examples among a range of rare diseases and syndromes affecting neuronal myelin. These disorders pose a significant burden on the people affected by them, as well as on our economy. For instance, a 2020 study reported a pooled incidence rate across 75 countries of 2.1 per 100,000 persons per year for multiple sclerosis [21]. Moreover, another study by Paz-Zulueta *et al.* (2020) [22] estimates the total annual cost per MS patient in Europe to average around 40,300 euros. Other neurological disorders, including schizophrenia and bipolar disorder, have also been associated with a dysregulated axo-myelin unit [23]. Hence, the incorporation of intra-axonal heterogeneity in studies modeling AP propagation in myelinated axons can boost our knowledge of the mechanisms behind these diseases and provide new insights into potential therapeutic targets, a crucial step towards the development of effective treatment approaches.

2 Methods

2.1 Model & Parameter Values

The double-cable model as developed by Richardson *et al.* (2000) [11] with the MATLAB implementation established by Arancibia-Cárcamo *et al.* (2017) [9] was used in our study. All simulations were performed in MATLAB version R2021a. The MATLAB implementation of the double-cable model can be freely downloaded from GitHub (`https://github.com/xmsterl/Project_group_`

2B). The parameter values were retrieved from the experimental results of Cullen *et al.* (2021) [16], where available. Only the periaxonal space width at the paranode and myelin wrap periodicity values were retrieved from Arancibia-Cárcamo *et al.* (2017) [9]. An overview of all parameter values used in the simulations can be found in Table S1.

2.2 Simulating Intra-Axonal Heterogeneity

The internode length, myelin thickness, and periaxonal space width were first varied separately among the internodes in the model in order to investigate the effect of intra-axonal heterogeneity. Moreover, to explore the combined effect of variable myelination, an additional simulation including intra-axonal variation of all three parameter values together was performed. All other parameters were assumed to be constant in each simulation. Figure 2 visually displays the constant and variable geometric parameters of a single internode in the model.

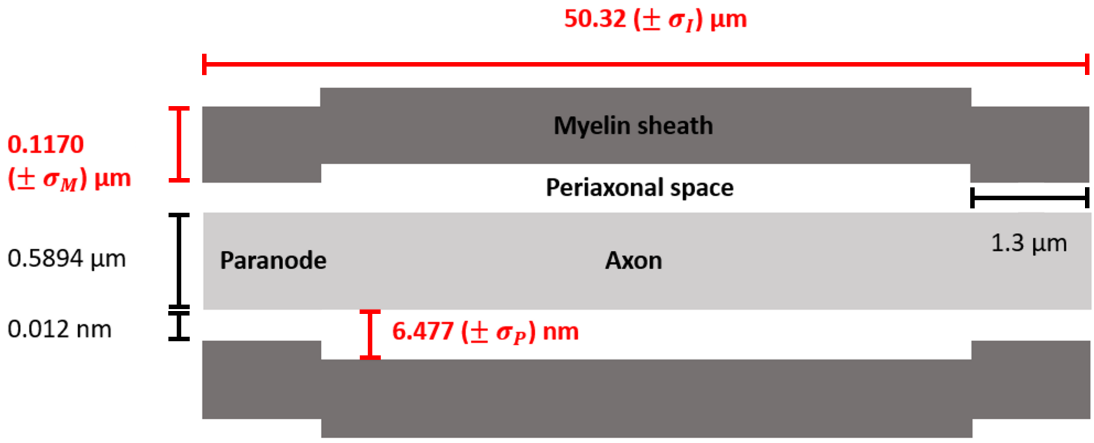

Figure 2: *Visual overview of an internode and the corresponding geometric neuron parameters used in the study. The parameter values colored in red were varied along the length of the axon.*

The internode length, myelin thickness, and periaxonal space width were varied around the mean according to four distinct coefficients of variation (CoefVar): 0.1, 0.2, 0.3, and the biological CoefVar as estimated from the experimental results of Cullen *et al.* (2021) [16]. The estimated biological CoefVar of the internode length, myelin thickness, and periaxonal space width are 0.10, 0.34, and 0.15, respectively. The variation of the parameter values along the axon was assumed to be normally distributed. Since intra-axonal variation was implemented using a random number generator, the model outcomes are not deterministic. Hence, 10 simulations per condition were performed to estimate the effect of intra-axonal heterogeneity on the AP conduction (Table 1). To ensure sufficient spatial resolution for each simulation with varying internode sizes, the maximum internode segment size was set to 0.8 μm, where the conduction velocity has converged to a stable value (Figure S1).

Table 1: Overview of the number of simulations per condition.

	Internode length	*Myelin thickness*	*Periaxonal space width*	*All*	**Sum**
CoefVar = 0.1	10	10	10	10	40
CoefVar = 0.2	10	10	10	10	40
CoefVar = 0.2	10	10	10	10	40
Biological CoefVar	10	10	10	10	40
Sum	40	40	40	40	160

2.3 Data Analysis

For each simulation, the mean and standard deviation of the voltage peak values of nodes 15 to 35 were calculated. The voltage peak value of a node is defined to be the maximum voltage value reached after the induction of a single axonal AP. Furthermore, the conduction velocity between nodes 15 and 35 was computed with the `velocities()` function available in the MATLAB implementation of the double-cable model. A two-sided one-sample t-test was performed to compare the mean voltage peak value and conduction velocity of the simulations with intra-axonal variation against the deterministic outcomes of the simulation without any intra-axonal variation. A Bonferroni-adjusted p-value ≤ 0.05 was considered to be statistically significant.

Principal component analysis (PCA) was performed to investigate the main sources of variation in the AP conduction between the different simulations. The voltage traces of nodes 15 to 35 over all time points were used as features in the PCA model.

3 Results

3.1 Intra-axonal variation reduces AP velocity and amplitude

As shown in Figure 3, intra-axonal variation in periaxonal space width, myelin thickness, and internode length alone do not lead to a significantly changed conduction velocity or mean voltage peak value. Nonetheless, varying all parameter values together along the axon resulted in a significantly reduced conduction velocity (adj. p-value = 0.013) and average voltage peak value (adj. p-value = 0.009) for a biological CoefVar. Furthermore, introducing heterogeneity of all parameter values along the axon with a CoefVar of 0.2 and a CoefVar of 0.3 only led to a lower conduction velocity (adj. p-values of 0.032 and 0.005, respectively) without a significant change in the average voltage peak value. Of note, although the conduction velocity and average voltage peak value are not significantly reduced for a variable myelin thickness, a negative relationship with the CoefVar can be observed in Figure 3.

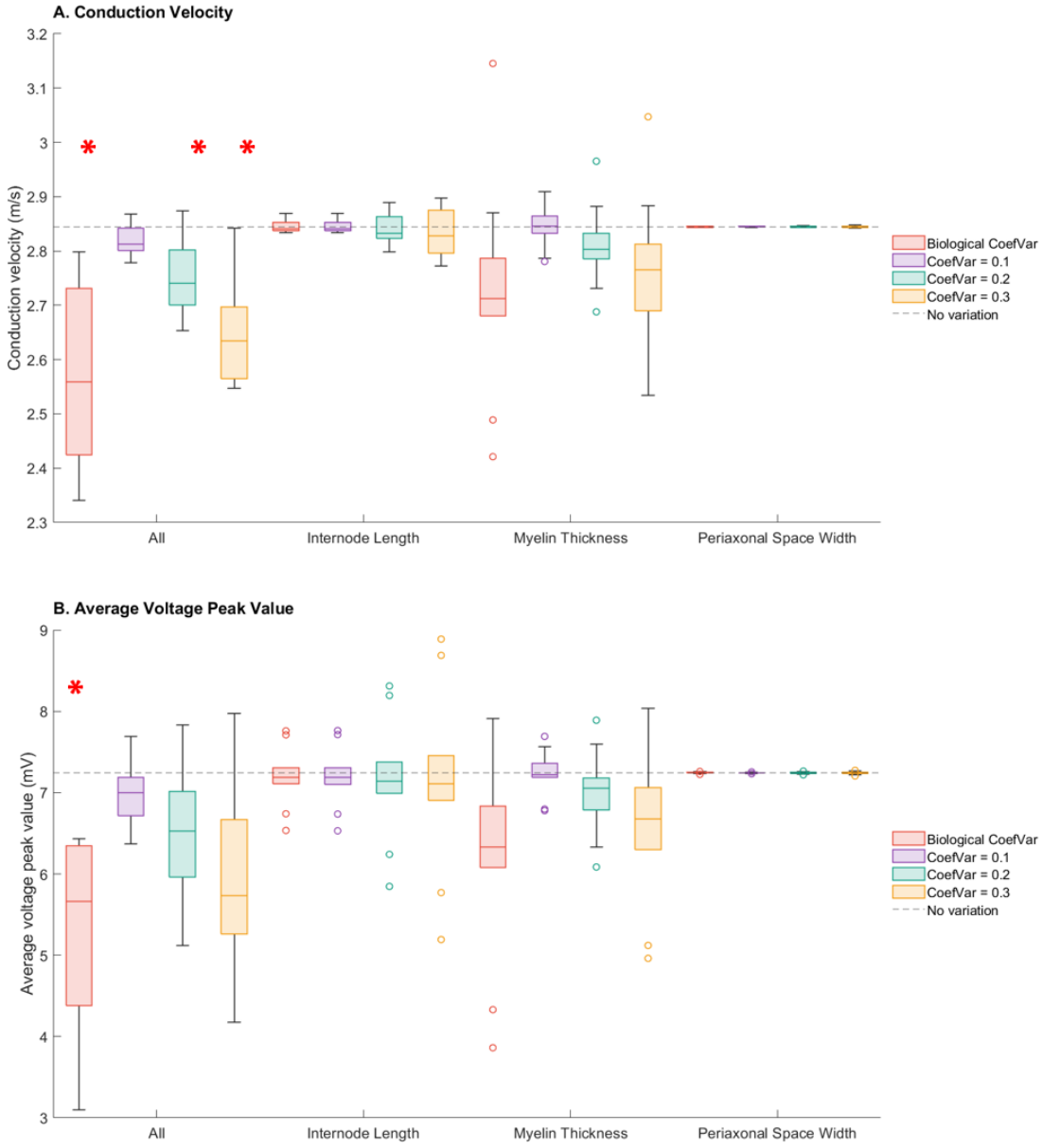

Figure 3: *Conduction velocity (**A**) and average voltage peak value (**B**) for the different simulations. The red * indicates a statistically significant difference from the simulation without variation (dashed line).*

3.2 Mean voltage peak value correlates with the main source of variation

Furthermore, PCA was performed to find the main sources of variation. The first principal component explains more than 75 % of the variance and is highly correlated with the average voltage peak value (r = 0.79) (Figure 4). However, PC1 does not seem to be correlated with any of the varied parameters (Figures 4 and S2). Interestingly, there is also a high correlation between conduction velocity and average voltage peak value (r = 0.80).

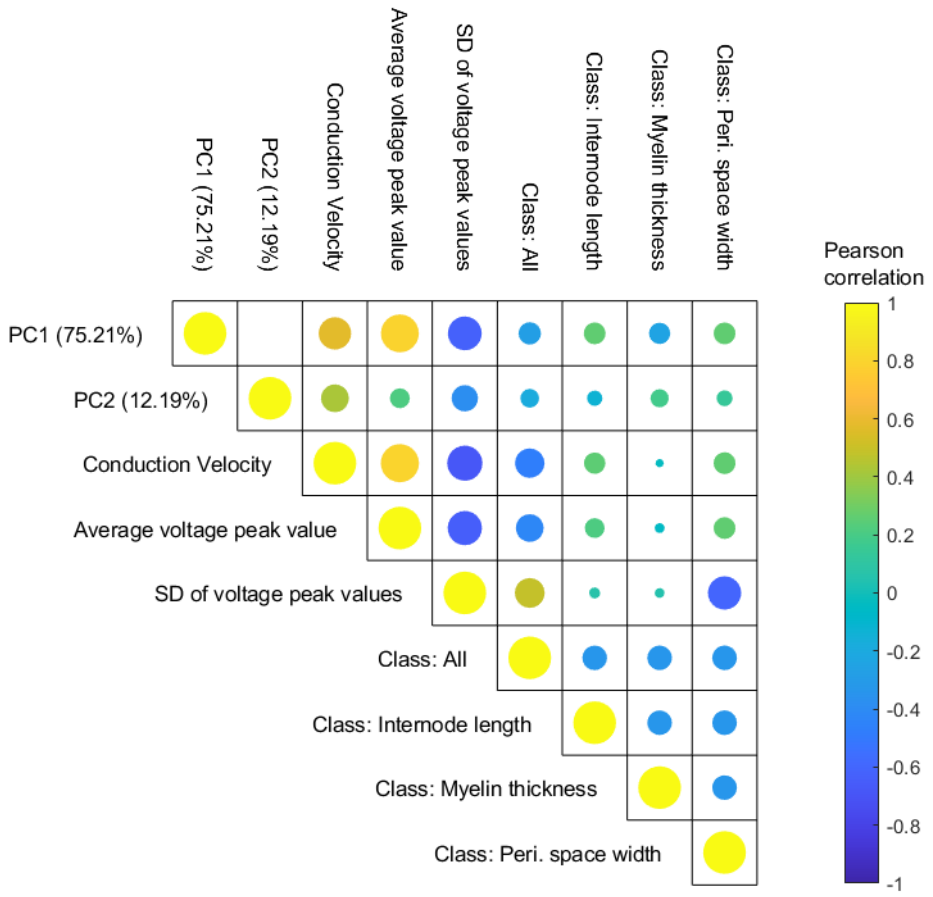

Figure 4: *Correlation plot of the pairwise correlations between the first and second principal components, AP velocity and amplitude (mean and standard deviation), and the parameter classes. The size of the dots correlates with the absolute Pearson correlation coefficient.*

3.3 Relationship between AP velocity and mean peak value

Figure 5 shows the relationship between conduction velocity and average voltage peak value. Interestingly, introducing intra-axonal heterogeneity in internode length led to inter-simulation variation in the mean voltage peak value without affecting the conduction velocity (Figures 5A and C). In contrast, there is a strong relationship between conduction velocity and mean voltage peak value when varying the myelin thickness along the axon (Figures 5A and D). Noteworthy, the variation in conduction velocity between the different simulations seems to be particularly related to the variation in mean internode length and myelin thickness (Figures 5C and D). Specifically, a smaller mean internode length is associated with an increase in the mean voltage peak value without affecting the conduction velocity, while a smaller myelin thickness is associated with a decrease in both the mean voltage peak value and conduction velocity.

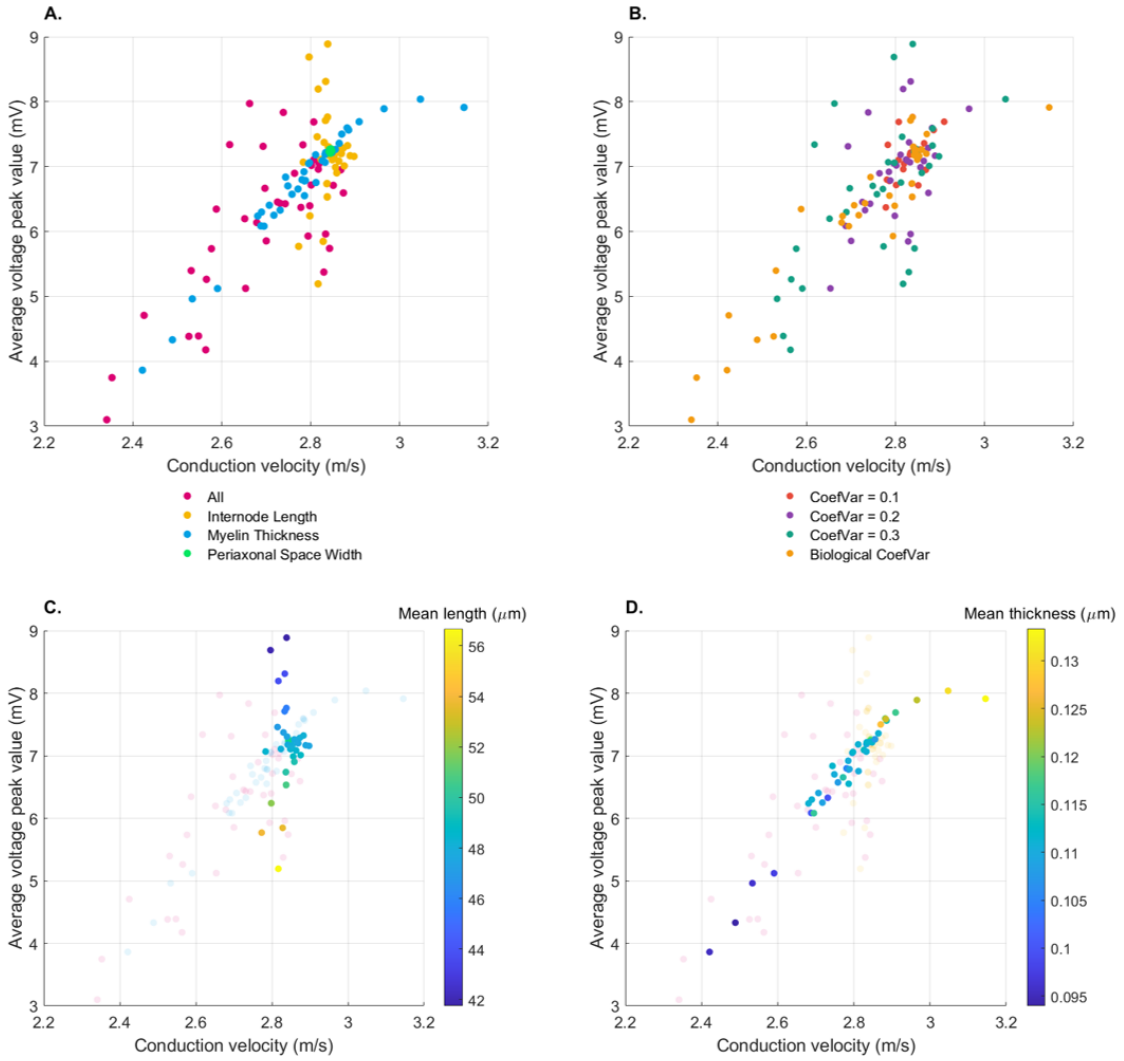

Figure 5: *Relationship between the conduction velocity and average voltage peak value. Data points (i.e., simulations) are colored by the parameter that is varied along the axon (**A**) and by the corresponding coefficient of variation (CoefVar) (**B**). Furthermore, a color gradient shows the mean internode length (**C**) and myelin thickness (**D**) for the simulations with a variable internode length and myelin thickness, respectively.*

4 Discussion

4.1 The impact of intra-axonal heterogeneity on AP conduction

Experimental studies have shown that various myelination parameters including myelin sheath length [15] and myelin thickness [20] are not homogeneously distributed along the axon. By incorporating different levels of intra-axonal heterogeneity into the double-cable model, we have shown that combined intra-axonal variability in internode length, myelin thickness, and periaxonal space width significantly reduces the AP velocity and amplitude (Figure 3). Interestingly, early modeling studies have shown that the conduction velocity decreases more steeply when the myelin thickness becomes smaller [24]. The internodes with a small myelin thickness might therefore act as a bottleneck for conduction velocity along a heterogeneously myelinated axon. This would

also explain why we observed a lower conduction velocity for a larger CoefVar of the myelin thickness. A similar non-linear relationship between myelin thickness and AP amplitude could possibly explain the observed lower average voltage peak value in the heterogeneously myelinated axon. However, the relationship between myelin thickness and AP amplitude has to our knowledge not been established yet.

It should be noted that the parameters we varied along the axon are not the only parameters that have been observed to vary along a single axon. For instance, Giacci *et al.* (2018) demonstrated that the axonal diameter, cross-sectional area, and myelin decompaction can also vary significantly along the axon of a retinal ganglion cell [20]. In addition, Arancibia-Cárcamo *et al.* (2017) found intra-axonal heterogeneity of the length of the node of Ranvier along the axons in the corpus callosum [9]. It is yet unknown how these additional sources of variation can affect AP propagation. Hence, it is up to future studies to investigate whether the incorporation of these additional sources of variation into the double-cable model limits or exaggerates the observed reduction in the conduction velocity and AP amplitude.

4.2 Myelination as a regulator of AP propagation

As an additional result, we have found that the average voltage peak value highly correlates with the main source of variation (Figure 4). Interestingly, inter-simulation differences in the average voltage peak value and conduction velocity were shown to be particularly explained by the variation in the mean internode length and myelin thickness (Figure 5), and thus not by the inter-simulation differences in the parameter distribution along the axon. These findings would suggest that changing the distribution of myelination along the axon is not as effective for the dynamic regulation of action potential conduction compared to dynamically altering the mean level of myelination along the axon. Indeed, the myelin distribution profile along the axon has previously been shown to follow a specific gradient in neurons of the auditory system [15] and the corpus callosum [25]. Additionally, the myelination distribution of an axon has been demonstrated to be specific for the neocortical layer of the neuron [19]. This may indicate that the global myelination distribution along an axon is a stable feature of a neuron and is thus not subject to large dynamical changes over time. Instead, myelination has been suggested to be locally fine-tuned for the regulation of axonal AP propagation [26]. Noteworthy, the notion that the global distribution of axonal myelination is not subject to dynamic alterations does not mean that it does not have a function in the regulation of AP conduction. Instead, in a study by Salami *et al.* (2003), it was observed that AP propagation along the axon of the neurons in the ventrobasal nucleus slows down when the axons enter the cortex as a result of the poor myelination in the cortical region [27]. The authors suggested that differences in the myelination along the axon serve as a regulatory mechanism to ensure that the timing of APs from multiple sources arrive within a

specific temporal window.

Furthermore, we have shown that a lower mean internode length is associated with a higher mean AP amplitude without affecting the conduction velocity (Figures 5A and C). These findings might be similar to findings by Ford *et al.* (2015) [15]. Their study demonstrated that a larger ratio of internode length to axon diameter decreased the AP amplitude. The proposed explanation is that increasing the internode length while keeping the axonal diameter constant will result in a less efficient transfer of current from one node to the adjacent one, which in turn leads to reduced synchronicity in the activation of Na^+ channels, and less rapid and synchronous activation of K^+ channels. By increasing the amplitude of APs, the reliability of AP propagation is increased. In addition, in line with our findings, early modeling studies also demonstrated the relative insensitivity of conduction velocity to changing internode length [28].

Finally, we have also found that a larger mean myelin thickness is associated with an increase in both the conduction velocity and the mean AP amplitude (Figures 5A and C). Ford *et al.* (2015) showed that by increasing the number of myelin wraps, thus the myelin thickness, the capacitance along the internode is lowered [15]. This results in the reduction of the time required to charge the internodal membrane, meaning that consecutive nodes of Ranvier require less time to reach their threshold value, thus increasing conduction velocity [15, 28]. Additionally, our findings are further supported by an experimental study by Barak *et al.* (2019) [29]. Specifically, in this study, it was shown that a reduced myelin thickness of neurons in the corpus callosum of *Gtf2i* knock-out mice is indeed associated with a reduction in both the axonal conductivity and the AP amplitude.

4.3 Insights & Implications

Most neuronal modeling approaches have, until now, ignored the presence of intra-axonal heterogeneity. However, our study has demonstrated that neglecting variation along the axon might lead to the overestimation of the AP conduction velocity and amplitude. Neuronal models that assume a homogeneous distribution of myelin along the axon are widely used in the scientific field: from bio-engineering [30] to more fundamental neurological research [16]. The new insights provided by our study may thus have implications for multiple scientific domains. In fact, accurate prediction of AP propagation is an essential aspect of computational approaches that try to simulate neuronal communication, synchronization, and information transmission. This becomes particularly relevant when considering studies that use neuronal models to simulate the effect of dys- and demyelinating disorders as well as other pathological conditions that are known to be associated with an exaggerated variability in myelination along the axon.

Moreover, our findings might also be of relevance for the development of new treatment approaches for dys- and demyelinating diseases. Particularly, remyelination therapeutics are considered to be promising treatment approaches for these diseases [31]. These promising remyelination

compounds (*e.g.*, modulators of sphingosine-1-phosphate receptor pathway) either stimulate oligodendrocyte precursor cell proliferation and differentiation, or promote the formation of myelin by mature oligodendrocytes [31]. Our results suggest that, for these remyelination compounds, increasing the mean myelination level along the axon alone might not be sufficient to re-establish healthy action potential conduction. Instead, minimizing intra-axonal variability would possibly also be required to fully restore axonal AP conductivity.

4.4 Future Computational Research

In the present study, we investigated the effect of intra-axonal variation on action potential conduction by imposing a random distribution of myelination parameter values along the axon. The proposed model establishes this biological variation in axon and myelin structure as Gaussian noise using experimentally derived distribution parameters, making it incredibly simple to implement, also into other existing models. Additionally, the model still allows for noise-free, detailed testing of the specific influence of individual parameters by setting the CoefVar equal to zero, as has been done by Blades *et al.* (2022) [32]. Future studies on the effect of axonal structure disruptions, for example, in de- or dysmyelinating disorders, could make use of the model by using distinct Gaussian distributions with parameter values for healthy and diseased states.

Including variation in the model more closely captures the physiological structures emerging from biological processes. Specifically, the incorporation of noise addresses the suggested intra-axonal variation in myelin sheath length resulting from initial myelination and myelin remodeling [18]. Nevertheless, in reality, the parameter values might not be completely randomly distributed along the axon. For example, a progressively increasing internode length along the axon has previously been observed in neurons of the auditory system [15]. Also, a myelination gradient in the corpus callosum has been detected in prior research [25]. Future studies could therefore investigate the effect of such a non-random distribution of myelination parameters along the axonal length on the AP conduction.

Moreover, the model used in the present study made use of multiple physiological simplifications that could be addressed in future computational modeling studies to make the model more biologically accurate. For instance, the current model did not include the voltage-gated potassium Kv1 channels that are enriched in the juxtaparanode, the region directly adjacent to the paranodal region. These juxtaparanodal Kv1 channels are thought to be important for the maintenance of the resting potential in the internodes [1]. Although these Kv1 channels are often thought to have little effect on AP conduction, no modeling study has, to our knowledge, investigated the effect of these ion channels on AP propagation along a (heterogeneously) myelinated axon. Incorporation of the juxtaparanodal Kv1 channels in future studies could make the model more biologically accurate.

In addition, we modeled the behavior of a single axon in isolation. Simulations by Blades *et al.* [32] have shown that changes in the AP propagation of a single axon do not necessarily translate into altered behavior of the signal conduction in nerve bundles (*e.g.*, compound action potentials). Future modeling studies could therefore investigate whether the reduction in AP conduction velocity and amplitude are also persistent at a higher anatomical scale (*e.g.*, nerve bundles).

4.5 Future Experimental Research

Similar to the present research, future modeling studies would require an experimental estimation of the biological variation along a single axon. However, the limited number of structural parameters measured in *in-vivo* neurobiological studies greatly restricts the current use of the model to only a few parameters, for which paired values for mean and standard deviation are available. Additionally, parameters are commonly measured in sections of a single brain area, and along numerous neurons, as has been done in the study by Cullen *et al.* (2021) from which the values for the mean and standard deviation of the myelin thickness, periaxonal space width, and internode length used in this study were taken. Interestingly, Arancibia-Cárcamo *et al.* (2017) found that the variation of the node length along a single axon is lower than the variation between axons. This would suggest that using the variation of myelination parameters measured from a single brain region may overestimate the true biological variability that occurs along a single axon.

In addition, prior studies that focused on estimating the variation along a single axon have mainly been estimating the variation of just a single parameter. For example, Arancibia-Cárcamo *et al.* (2017) estimated the intra-axonal variation of node length in the optic nerve of rats [9], while Call and Bergles (2021) investigated the heterogeneity of the internode length along the axons in the somatosensory cortex of mice [33]. The different organisms and tissues from which the single parameter values are estimated make it very difficult to integrate these values into a single neuronal model. Hence, a possible direction for future research would be to estimate the intra-axonal variation for multiple (myelination) parameters per tissue and organism. Using the estimated parameters, future computational modeling studies could more reliably investigate the effects of intra-axonal heterogeneity on AP propagation.

5 Conclusion

In conclusion, in this study we propose new insights into the mechanisms underlying AP propagation by introducing structural variation of myelin sheaths in a computational model representing the axon-myelin unit. In particular, we have shown that this heterogeneity has a clear impact on neuronal properties, specifically, a significant reduction of the AP amplitude and conduction veloc-

ity. By updating the previously formulated double-cable model, we provide a new framework for more biologically accurate studies regarding the effect of an irregular distribution of myelin. These results will prove to be useful not only in healthy states, but even more in diseased conditions, where this irregularity is enhanced. As a final remark, while more work is needed to determine precise ranges of values for the parameters under consideration and to identify variation at the neuronal population level, our research represents a first important step in this direction.

References

1. Arancibia-Carcamo, I. L. & Attwell, D. The node of Ranvier in CNS pathology. *Acta Neuropathologica* **128,** 161–175 (2014).
2. Susuki, K. Node of Ranvier Disruption as a Cause of Neurological Diseases. *ASN Neuro* **5,** AN20130025 (2013).
3. Poliak, S. & Peles, E. The local differentiation of myelinated axons at nodes of Ranvier. *Nature Reviews Neuroscience* **4,** 968–980 (2003).
4. Nave, K.-A. & Werner, H. B. Myelination of the Nervous System: Mechanisms and Functions. *Annual Review of Cell and Developmental Biology* **30,** 503–533 (2014).
5. Dutta, D. J. *et al.* Regulation of myelin structure and conduction velocity by perinodal astrocytes. *Proceedings of the National Academy of Sciences* **115,** 11832–11837 (2018).
6. Barrett, E. F. & Barrett, J. N. Intracellular recording from vertebrate myelinated axons: mechanism of the depolarizing afterpotential. *The Journal of physiology* **323,** 117–144 (1982).
7. Blight, A. & Someya, S. Depolarizing afterpotentials in myelinated axons of mammalian spinal cord. *Neuroscience* **15,** 1–12 (1985).
8. Funch, P. G. & Faber, D. S. Measurement of myelin sheath resistances: implications for axonal conduction and pathophysiology. *Science* **225,** 538–540 (1984).
9. Arancibia-Cárcamo, I. L. *et al.* Node of Ranvier length as a potential regulator of myelinated axon conduction speed. *Elife* **6,** e23329 (2017).
10. Blight, A. Computer simulation of action potentials and afterpotentials in mammalian myelinated axons: the case for a lower resistance myelin sheath. *Neuroscience* **15,** 13–31 (1985).
11. Richardson, A., McIntyre, C. & Grill, W. Modelling the effects of electric fields on nerve fibres: influence of the myelin sheath. *Medical and Biological Engineering and Computing* **38,** 438–446 (2000).
12. Cohen, C. C. *et al.* Saltatory conduction along myelinated axons involves a periaxonal nanocircuit. *Cell* **180,** 311–322 (2020).
13. McNeal, D. R. Analysis of a model for excitation of myelinated nerve. *IEEE Transactions on Biomedical Engineering,* 329–337 (1976).
14. Halter, J. A. & Clark Jr, J. A distributed-parameter model of the myelinated nerve fiber. *Journal of theoretical biology* **148,** 345–382 (1991).
15. Ford, M. C. *et al.* Tuning of Ranvier node and internode properties in myelinated axons to adjust action potential timing. *Nature communications* **6,** 1–14 (2015).
16. Cullen, C. L. *et al.* Periaxonal and nodal plasticities modulate action potential conduction in the adult mouse brain. *Cell Reports* **34,** 108641 (2021).

17. Castelfranco, A. M. & Hartline, D. K. The evolution of vertebrate and invertebrate myelin: a theoretical computational study. *Journal of computational neuroscience* **38,** 521–538 (2015).

18. Auer, F., Vagionitis, S. & Czopka, T. Evidence for myelin sheath remodeling in the CNS revealed by in vivo imaging. *Current Biology* **28,** 549–559 (2018).

19. Tomassy, G. S. *et al.* Distinct profiles of myelin distribution along single axons of pyramidal neurons in the neocortex. *Science* **344,** 319–324 (2014).

20. Giacci, M. K. *et al.* Three dimensional electron microscopy reveals changing axonal and myelin morphology along normal and partially injured optic nerves. *Scientific reports* **8,** 1–12 (2018).

21. Walton, C. *et al.* Rising prevalence of multiple sclerosis worldwide: Insights from the Atlas of MS, third edition. *Multiple Sclerosis Journal* **26,** 1816–1821 (2020).

22. Paz-Zulueta, M., Parás-Bravo, P., Cantarero-Prieto, D., Blázquez-Fernández, C. & Oterino-Durán, A. A literature review of cost-of-illness studies on the economic burden of multiple sclerosis. *Multiple Sclerosis and Related Disorders* **43,** 102162 (2020).

23. Valdés-Tovar, M. *et al.* Insights into myelin dysfunction in schizophrenia and bipolar disorder. *World Journal of Psychiatry* **12,** 264 (2022).

24. Waxman, S. G. Determinants of conduction velocity in myelinated nerve fibers. *Muscle & Nerve: Official Journal of the American Association of Electrodiagnostic Medicine* **3,** 141–150 (1980).

25. Friedrich, P. *et al.* The relationship between axon density, myelination, and fractional anisotropy in the human corpus callosum. *Cerebral Cortex* **30,** 2042–2056 (2020).

26. Suminaite, D., Lyons, D. A. & Livesey, M. R. Myelinated axon physiology and regulation of neural circuit function. *Glia* **67,** 2050–2062 (2019).

27. Salami, M., Itami, C., Tsumoto, T. & Kimura, F. Change of conduction velocity by regional myelination yields constant latency irrespective of distance between thalamus and cortex. *Proceedings of the National Academy of Sciences* **100,** 6174–6179 (2003).

28. Moore, J. W., Joyner, R. W., Brill, M. H., Waxman, S. D. & Najar-Joa, M. Simulations of conduction in uniform myelinated fibers. Relative sensitivity to changes in nodal and internodal parameters. *Biophysical journal* **21,** 147–160 (1978).

29. Barak, B. *et al.* Neuronal deletion of Gtf2i, associated with Williams syndrome, causes behavioral and myelin alterations rescuable by a remyelinating drug. *Nature neuroscience* **22,** 700–708 (2019).

30. Ye, S., Zhu, K., Li, P. & Sui, X. Neural Firing Mechanism Underlying Two-Electrode Discrimination by 3D Transcutaneous Electrical Nerve Stimulation Computational Model. *Journal of Shanghai Jiaotong University (Science)* **24,** 716–722 (2019).

31. Lubetzki, C., Zalc, B., Williams, A., Stadelmann, C. & Stankoff, B. Remyelination in multiple sclerosis: from basic science to clinical translation. *The Lancet Neurology* **19,** 678–688 (2020).

32. Blades, F. *et al.* White matter tract conductivity is resistant to wide variations in paranodal structure and myelin thickness accompanying the loss of Tyro3: an experimental and simulated analysis. *Brain Structure and Function,* 1–14 (2022).

33. Call, C. L. & Bergles, D. E. Cortical neurons exhibit diverse myelination patterns that scale between mouse brain regions and regenerate after demyelination. *Nature communications* **12,** 1–15 (2021).

34. Morton, J. T. *et al.* Uncovering the horseshoe effect in microbial analyses. *Msystems* **2,** e00166–16 (2017).

Supplementary Material

Table S1: Parameter values

Parameter	Value
Temperature	37 °C
dt	0.05 μs
tmax	2 ms
Stimulation amplitude	0.5 nA
Stimulation duration	10 μs
Number of nodes	51
Number of internodes	50
Axonal diameter	0.5894 μm
Node length	0.8364 μm
Internode length	N(50.32, 50.32*CoefVar) μm
Maximum internode segment length	0.8 μm
Paranode length	1.3 μm
Periaxonal space width	N(6.477, 6.477*CoefVar) nm
Periaxonal space width (at paranode)*	0.012 nm
Myelin wrap periodicity*	15.6 nm
Myelin Thickness	N(0.1170, 0.1170*CoefVar) μm
Number of myelin lamellae	Ceil(myelin width / wrap periodicity)
Resting membrane potential	-72 mV
Node leak reversal potential	-84 mV
Node axial resistivity	0.7 Ωm
Node membrane capacitance	0.9 μF / cm^2
Myelin membrane capacitance	0.9 μF / cm^2
Myelin membrane conductance	1 mS/ mm^2
Internode axon membrane capacitance	0.9 μF / cm^2
Internode axon membrane conductance	0.1 mS/ mm^2
Periaxonal space resistivity	0.7 Ωm

*Parameter value retrieved from Arancibia-Carcamo *et al.* (2017). All other parameter values were retrieved from Cullen *et al.* (2021).

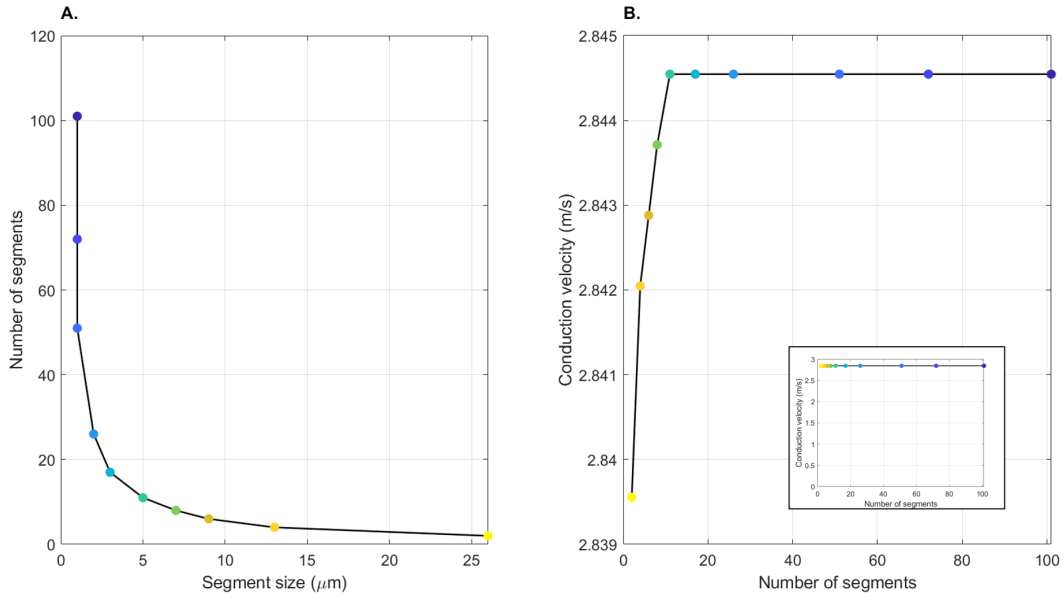

Figure S1: *Convergence of the conduction velocity. The graphs show the number of segments as function of segment size (**A**) and the conduction velocity as a function of the number of segments (**B**).*

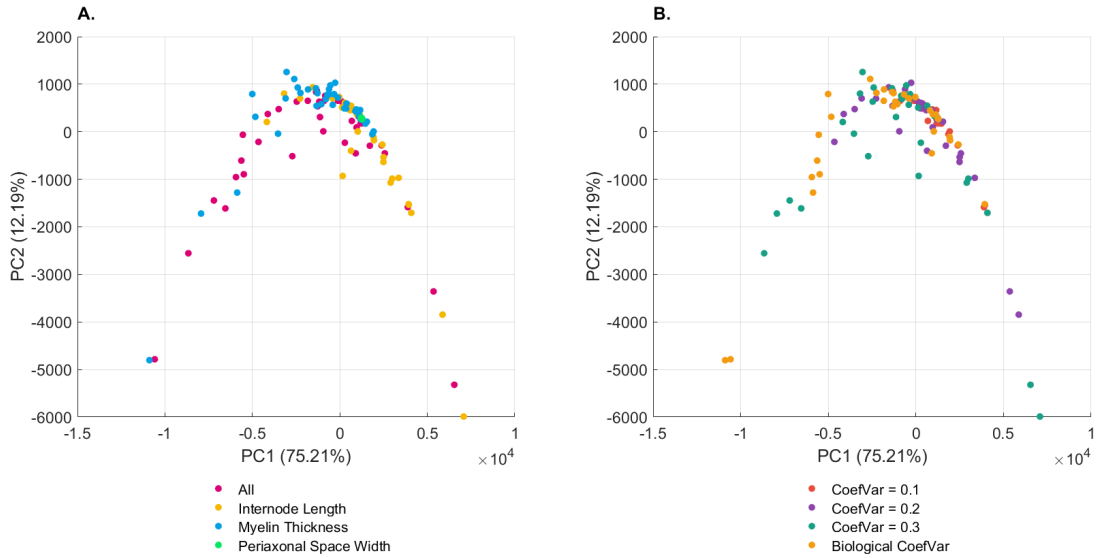

Figure S2: *Principal component analysis plot. The data points (i.e., simulations) are coloured by the parameter that is varied along the axon (**A**) and by the corresponding coefficient of variation (CoefVar) (**B**). The negative parabolic shape (*i.e., *Horseshoe effect) is the result of non-linear relationships between the variables, not captured by the PCA. [34]*